

# Exploring the evolution of color-luminosity parameter $\beta$ and its effects on parameter estimation

Shuang Wang,<sup>1,\*</sup> Yun-He Li,<sup>1,†</sup> and Xin Zhang<sup>1,2,‡</sup>

<sup>1</sup>*Department of Physics, College of Sciences, Northeastern University, Shenyang 110004, China*

<sup>2</sup>*Center for High Energy Physics, Peking University, Beijing 100080, China*

In Phys. Rev. D 88, 043511 (2013), using the Supernova Legacy Survey Three Year (SNLS3) data, Wang & Wang found that there is a strong evidence for the redshift-evolution of color-luminosity parameter  $\beta$ . In this paper, using three simplest dark energy models ( $\Lambda$ CDM,  $w$ CDM, and CPL), we further explore the evolution of  $\beta$  and its effects on parameter estimation. In addition to the SNLS3 data, we also take into account the Planck distance priors data, as well as the latest galaxy clustering (GC) data extracted from SDSS DR7 and BOSS. We find that, for all the models,  $\beta$  deviates from a constant at  $5\sigma$  confidence levels. Moreover, adding a parameter of  $\beta$  can reduce the best-fit values of  $\chi^2$  by  $\sim 35$ , showing the importance of considering the evolution of  $\beta$  in the cosmology-fits. We find that, using the SNLS3 data alone, varying  $\beta$  yields a larger  $\Omega_m$  for the  $\Lambda$ CDM model; using the SNLS3+CMB+GC data, varying  $\beta$  yields a larger  $\Omega_m$  and a smaller  $h$  for all the models. Moreover, we find that these results are much closer to those given by the CMB+GC data, compared to the cases of treating  $\beta$  as a constant. This indicates that considering the evolution of  $\beta$  is very helpful for reducing the tension between supernova and other cosmological observations.

PACS numbers: 98.80.-k, 98.80.Es, 95.36.+x

Keywords: Cosmology, type Ia supernova, dark energy

## I. INTRODUCTION

Various astronomical observations [1–7] all indicate that the Universe is undergoing an accelerated expansion. So far, we are still in the dark about the nature of this extremely counterintuitive phenomenon; it may be due to an unknown energy component (i.e., dark energy (DE) [8–19]), or a modification of general relativity (i.e., modified gravity (MG) [20–27]). For recent reviews, see [28–37].

One of the most powerful probes of DE is the use of type Ia supernovae (SNe Ia), which can be used as cosmological standard candles to measure the expansion history of the Universe. In recent years, several supernova (SN) datasets with hundreds of SNe Ia were released, such as “Union” [38], “Constitution” [39], “SDSS” [40], “Union2” [41] and “Union2.1” [42].

In 2010, a high quality SN dataset from the first three years of the Supernova Legacy Survey (SNLS3) was released [43]. Soon after, Conley et al. (2011; hereafter C11) presented SNe-only cosmological results by combining the SNLS3 SNe with various low- to mid- $z$  samples [44], and Sullivan et al. presented the joint cosmological constraints by combining the SNLS3 dataset with other cosmological data sets [45]. C11 presented three SNe data sets, depending on different light-curve fitters: “SALT2”, which consists of 473 SNe Ia; “SiFTO”, which consists of 468 SNe Ia; and “combined”, which consists of 472 SNe Ia. It should be stressed that, the SNLS team

treated two important quantities, stretch-luminosity parameter  $\alpha$  and color-luminosity parameter  $\beta$  of SNe Ia, as free model parameters on the same footing as the cosmological parameters, all to be estimated during the Hubble diagram fitting process using the covariance matrix that includes *both* statistical and systematic errors.

A critical challenge is the control of the systematic uncertainties of SNe Ia. One of the most important factors is the effect of potential SN evolution, i.e., the possibility of the evolution of  $\alpha$  and  $\beta$  with redshift  $z$ . So far,  $\alpha$  is still consistent with a constant, but the evolution of  $\beta$  has been found for both the SDSS [40] and the Union2.1 [46] SN samples. In [47], Wang & Wang studied this issue by using the SNLS3 data. They found no evidence for the evolution of  $\alpha$ , but  $\beta$  increases significantly with  $z$  when systematic uncertainties are taken into account. It should be stressed that, this conclusion is insensitive to the lightcurve fitter used to derive the SNLS3 sample, or the functional form of  $\beta(z)$  assumed [47].

It is clear that a time-varying  $\beta$  has significant impact on parameter estimation. In [47], using the cubic spline interpolation for a scaled comoving distance  $r_p(z)$ , Wang & Wang briefly discussed the effects of varying  $\beta$  on distance-redshift relation. It is also very interesting to study the impact of varying  $\beta$  on various cosmological models. So in this paper, we study this issue by considering three simplest DE models:  $\Lambda$ CDM,  $w$ CDM, and CPL [48]. For comparison, we also take into account the Planck distance priors data [49], as well as the latest galaxy clustering (GC) data extracted from SDSS DR7 [50] and BOSS [51].

We describe our method in Sec. II, present our results in Sec. III, and conclude in Sec. IV.

\*Electronic address: wjysygsj@163.com

†Electronic address: liyh19881206@126.com

‡Electronic address: zhangxin@mail.neu.edu.cn

## II. METHOD

The comoving distance to an object at redshift  $z$  is given by:

$$r(z) = cH_0^{-1} |\Omega_k|^{-1/2} \text{sinn}[\Omega_k^{1/2} \Gamma(z)], \quad (1)$$

$$\Gamma(z) = \int_0^z \frac{dz'}{E(z')}, \quad E(z) = H(z)/H_0$$

where  $\text{sinn}(x) = \sin(x)$ ,  $x$ ,  $\sinh(x)$  for  $\Omega_k < 0$ ,  $\Omega_k = 0$ , and  $\Omega_k > 0$  respectively. The expansion rate of the universe  $H(z)$  (i.e., the Hubble parameter) is given by

$$H^2(z) = H_0^2 [\Omega_m(1+z)^3 + \Omega_k(1+z)^2 + \Omega_X X(z)], \quad (2)$$

where  $\Omega_m + \Omega_k + \Omega_X = 1$ .  $\Omega_m$  also includes the contribution from massive neutrinos besides the contributions from baryons and dark matter; the dark energy density function  $X(z)$  is defined as

$$X(z) \equiv \frac{\rho_X(z)}{\rho_X(0)}. \quad (3)$$

Note that  $\Omega_{\text{rad}} = \Omega_m/(1+z_{\text{eq}}) \ll \Omega_m$  (with  $z_{\text{eq}}$  denoting the redshift at matter-radiation equality), thus the  $\Omega_{\text{rad}}$  term is usually omitted in dark energy studies at  $z \ll 1000$ , since dark energy should only be important at late times.

### A. SNe Ia Data

SNe Ia data give measurements of the luminosity distance  $d_L(z)$  through that of the distance modulus of each SN:

$$\mu_0 \equiv m - M = 5 \log \left[ \frac{d_L(z)}{\text{Mpc}} \right] + 25, \quad (4)$$

where  $m$  and  $M$  represent the apparent and absolute magnitude of an SN. The luminosity distance  $d_L(z) = (1+z)r(z)$ , with the comoving distance  $r(z)$  given by Eq. (1).

Here we use the SNLS3 data set. As mentioned above, based on different light-curve fitters, three SNe sets of SNLS3 are given, including ‘‘SALT2’’, ‘‘SiFTO’’, and ‘‘combined’’. As shown in [47], the conclusion of evolution of  $\beta$  is insensitive to the lightcurve fitter used to derive the SNLS3 sample. So in this paper we just use the ‘‘combined’’ set.

In [47], by considering three functional forms (linear case, quadratic case, and step function case), Wang & Wang explored the possible evolution of  $\alpha$  and  $\beta$ . It is found that  $\alpha$  is still consistent with a constant, but  $\beta$  increases significantly with  $z$ . It should be stressed that this conclusion is insensitive to functional form of  $\alpha$  and  $\beta$  assumed [47]. So in this paper, we just adopt a constant  $\alpha$  and a linear  $\beta(z) = \beta_0 + \beta_1 z$ . Now, the predicted magnitude of an SN becomes,

$$m_{\text{mod}} = 5 \log_{10} \mathcal{D}_L(z|\mathbf{p}) - \alpha(s-1) + \beta(z)\mathcal{C} + \mathcal{M}, \quad (5)$$

where  $\mathcal{D}_L(z|\mathbf{p})$  is the luminosity distance multiplied by  $H_0$  for a given set of cosmological parameters  $\{\mathbf{p}\}$ ,  $s$  is the stretch measure of the SN light curve shape, and  $\mathcal{C}$  is the color measure for the SN.  $\mathcal{M}$  is a nuisance parameter representing some combination of the absolute magnitude of a fiducial SN,  $M$ , and the Hubble constant,  $H_0$ . Since the time dilation part of the observed luminosity distance depends on the total redshift  $z_{\text{hel}}$  (special relativistic plus cosmological), we have

$$\mathcal{D}_L(z|\mathbf{s}) \equiv c^{-1} H_0 (1+z_{\text{hel}}) r(z|\mathbf{s}), \quad (6)$$

where  $z$  and  $z_{\text{hel}}$  are the CMB restframe and heliocentric redshifts of the SN.

For a set of  $N$  SNe with correlated errors, we have [44]

$$\chi^2 = \Delta \mathbf{m}^T \cdot \mathbf{C}^{-1} \cdot \Delta \mathbf{m} \quad (7)$$

where  $\Delta \mathbf{m} \equiv m_B - m_{\text{mod}}$  is a vector with  $N$  components,  $m_B$  is the rest-frame peak B-band magnitude of the SN, and  $\mathbf{C}$  is the  $N \times N$  covariance matrix of the SN. Note that  $\Delta \mathbf{m}$  is equivalent to  $\Delta \mu_0$ , since

$$\Delta \mathbf{m} \equiv m_B - m_{\text{mod}} = [m_B + \alpha(s-1) - \beta(z)\mathcal{C}] - \mathcal{M}. \quad (8)$$

The total covariance matrix is [44]

$$\mathbf{C} = \mathbf{D}_{\text{stat}} + \mathbf{C}_{\text{stat}} + \mathbf{C}_{\text{sys}}, \quad (9)$$

with the diagonal part of the statistical uncertainty given by [44]

$$\begin{aligned} \mathbf{D}_{\text{stat},ii} &= \sigma_{m_B,i}^2 + \sigma_{\text{int}}^2 + \sigma_{\text{lensing}}^2 + \sigma_{\text{host correction}}^2 \\ &+ \left[ \frac{5(1+z_i)}{z_i(1+z_i/2) \ln 10} \right]^2 \sigma_{z,i}^2 \\ &+ \alpha^2 \sigma_{s,i}^2 + \beta(z_i)^2 \sigma_{\mathcal{C},i}^2 \\ &+ 2\alpha C_{m_B s,i} - 2\beta(z_i) C_{m_B \mathcal{C},i} \\ &- 2\alpha\beta(z_i) C_{s \mathcal{C},i}, \end{aligned} \quad (10)$$

where  $C_{m_B s,i}$ ,  $C_{m_B \mathcal{C},i}$ , and  $C_{s \mathcal{C},i}$  are the covariances between  $m_B$ ,  $s$ , and  $\mathcal{C}$  for the  $i$ -th SN,  $\beta_i = \beta(z_i)$  are the values of  $\beta$  for the  $i$ -th SN. Note also that  $\sigma_{z,i}^2$  includes a peculiar velocity residual of 0.0005 (i.e., 150 km/s) added in quadrature [44]. Per C11, here we fix the intrinsic scatter  $\sigma_{\text{int}}$  to ensure that  $\chi^2/dof = 1$ . Varying  $\sigma_{\text{int}}$  could have a significant impact on parameter estimation, see [52] for details.

We define  $\mathbf{V} \equiv \mathbf{C}_{\text{stat}} + \mathbf{C}_{\text{sys}}$ , where  $\mathbf{C}_{\text{stat}}$  and  $\mathbf{C}_{\text{sys}}$  are the statistical and systematic covariance matrices, respectively. After treating  $\beta$  as functions of  $z$ ,  $\mathbf{V}$  is given in the form:

$$\begin{aligned} \mathbf{V}_{ij} &= V_{0,ij} + \alpha^2 V_{a,ij} + \beta_i \beta_j V_{b,ij} \\ &+ \alpha V_{0a,ij} + \alpha V_{0a,ji} \\ &- \beta_j V_{0b,ij} - \beta_i V_{0b,ji} \\ &- \alpha \beta_j V_{ab,ij} - \alpha \beta_i V_{ab,ji}. \end{aligned} \quad (11)$$

It must be stressed that, while  $V_0$ ,  $V_a$ ,  $V_b$ ,  $V_{0a}$ , are the same as the ‘‘normal’’ covariance matrices given by the

SNLS3 data archive,  $V_{0b}$ , and  $V_{ab}$  are *not* the same as the ones given there. This is because the original matrices of SNLS3 are produced by assuming that  $\beta$  is a constant. We have used the  $V_{0b}$ , and  $V_{ab}$  matrices for the “combined” set that are applicable when varying  $\beta(z)$  (A. Conley, private communication, 2013).

In [47], it is found that the flux-averaging of SNe [53–56] may be helpful to reduce the impact of varying  $\beta$ . It should be mentioned that, the results of flux-averaging depend on the choices of redshift cut-off  $z_{\text{cut}}$ :  $\beta$  still increases with  $z$  when all the SNe are flux-averaged, and  $\beta$  is consistent with being a constant when only SNe at  $z \geq 0.04$  are flux-averaged [47]. Since the unknown systematic biases originate mostly from low  $z$  SNe, flux-averaging *all* SNe should lead to the least biased results. Therefore, after applying the flux-averaging method, the problem of varying  $\beta$  is not completely solved. For simplicity, we do not use the flux-averaging method in this paper, and we will discuss the issue of flux-averaging in future work.

## B. CMB and GC data

For CMB data, we use the latest distance priors data extracted from Planck first data release [49].

CMB give us the comoving distance to the photon-decoupling surface  $r(z_*)$ , and the comoving sound horizon at photon-decoupling epoch  $r_s(z_*)$ . Wang & Mukherjee [57] showed that the CMB shift parameters

$$\begin{aligned} R &\equiv \sqrt{\Omega_m H_0^2} r(z_*)/c, \\ l_a &\equiv \pi r(z_*)/r_s(z_*), \end{aligned} \quad (12)$$

together with  $\omega_b \equiv \Omega_b h^2$ , provide an efficient summary of CMB data as far as dark energy constraints go. Replacing  $\omega_b$  with  $z_*$  gives identical constraints when the CMB distance priors are combined with other data [58]. Using  $\omega_b$ , instead of  $z_*$ , is more appropriate in a Markov Chain Monte Carlo (MCMC) analysis in which  $\omega_b$  is a base parameter.

The comoving sound horizon at redshift  $z$  is given by

$$\begin{aligned} r_s(z) &= \int_0^z \frac{c_s dt'}{a} = cH_0^{-1} \int_z^\infty dz' \frac{c_s}{E(z')}, \\ &= cH_0^{-1} \int_0^a \frac{da'}{\sqrt{3(1 + \bar{R}_b a') a'^4 E^2(z')}}}, \end{aligned} \quad (13)$$

where  $a$  is the cosmic scale factor,  $a = 1/(1+z)$ , and  $a^4 E^2(z) = \Omega_m(a + a_{\text{eq}}) + \Omega_k a^2 + \Omega_X X(z) a^4$ , with  $a_{\text{eq}} = \Omega_{\text{rad}}/\Omega_m = 1/(1+z_{\text{eq}})$ , and  $z_{\text{eq}} = 2.5 \times 10^4 \Omega_m h^2 (T_{\text{cmb}}/2.7 \text{ K})^{-4}$ . The sound speed is  $c_s = 1/\sqrt{3(1 + \bar{R}_b a)}$ , with  $\bar{R}_b a = 3\rho_b/(4\rho_\gamma)$ ,  $\bar{R}_b = 31500 \Omega_b h^2 (T_{\text{cmb}}/2.7 \text{ K})^{-4}$ . We take  $T_{\text{cmb}} = 2.7255 \text{ K}$ .

The redshift to the photon-decoupling surface,  $z_*$ , is

given by the fitting formula [59]:

$$z_* = 1048 [1 + 0.00124(\Omega_b h^2)^{-0.738}] [1 + g_1(\Omega_m h^2)^{g_2}], \quad (14)$$

where

$$g_1 = \frac{0.0783 (\Omega_b h^2)^{-0.238}}{1 + 39.5 (\Omega_b h^2)^{0.763}}, \quad (15)$$

$$g_2 = \frac{0.560}{1 + 21.1 (\Omega_b h^2)^{1.81}}. \quad (16)$$

The redshift of the drag epoch  $z_d$  is well approximated by [60]

$$z_d = \frac{1291(\Omega_m h^2)^{0.251}}{1 + 0.659(\Omega_m h^2)^{0.828}} [1 + b_1(\Omega_b h^2)^{b_2}], \quad (17)$$

where

$$b_1 = 0.313(\Omega_m h^2)^{-0.419} [1 + 0.607(\Omega_m h^2)^{0.674}], \quad (18)$$

$$b_2 = 0.238(\Omega_m h^2)^{0.223}. \quad (19)$$

Using the Planck+lensing+WP data, the mean values and covariance matrix of  $\{R, l_a, \omega_b\}$  are obtained [49],

$$\begin{aligned} \langle l_a \rangle &= 301.57, \sigma(l_a) = 0.18, \\ \langle R \rangle &= 1.7407, \sigma(R) = 0.0094, \\ \langle \omega_b \rangle &= 0.02228, \sigma(\omega_b) = 0.00030. \end{aligned} \quad (20)$$

The normalized covariance matrix of  $(l_a, R, \omega_b)$  is

$$\begin{pmatrix} 1.0000 & 0.5250 & -0.4235 \\ 0.5250 & 1.0000 & -0.6925 \\ -0.4235 & -0.6925 & 1.0000 \end{pmatrix}. \quad (21)$$

Then, the covariance matrix for  $(l_a, R, \omega_b)$  is given by

$$\text{Cov}_{CMB}(p_i, p_j) = \sigma(p_i) \sigma(p_j) \text{NormCov}_{CMB}(p_i, p_j), \quad (22)$$

where  $i, j = 1, 2, 3$ . The rms variance  $\sigma(p_i)$  and the normalized covariance matrix  $\text{NormCov}_{CMB}$  are given by Eqs. (20) and (21).

CMB data are included in our analysis by adding the following term to the  $\chi^2$  of a given model with  $p_1 = l_a(z_*)$ ,  $p_2 = R(z_*)$ , and  $p_3 = \omega_b$ :

$$\chi_{CMB}^2 = \Delta p_i [\text{Cov}_{CMB}^{-1}(p_i, p_j)] \Delta p_j, \quad \Delta p_i = p_i - p_i^{\text{data}}, \quad (23)$$

where  $p_i^{\text{data}}$  are the mean from Eq. (20), and  $\text{Cov}_{CMB}^{-1}$  is the inverse of the covariance matrix of  $[l_a(z_*), R(z_*), \omega_b]$  from Eq. (22).

For GC data, we use the measurements of  $H(z)r_s(z_d)/c$  and  $D_A(z)/r_s(z_d)$  (where  $H(z)$  is the Hubble parameter,  $D_A(z)$  is the angular diameter distance, and  $r_s(z_d)$  is the sound horizon at the drag epoch) from the two-dimensional two-point correlation function measured at  $z = 0.35$  [50] and  $z = 0.57$  [51]. The  $z = 0.35$  measurement was made by Chuang & Wang [50] using a sample of the SDSS DR7 Luminous Red Galaxies (LRGs). The

$z = 0.57$  measurement was made by Chuang et al. [51] using the CMASS galaxy sample from BOSS.

Using the two-dimensional two-point correlation function of SDSS DR7 in the scale range of 40–120 Mpc/ $h$ , Chuang & Wang [50] found that

$$\begin{aligned} H(z = 0.35)r_s(z_d)/c &= 0.0434 \pm 0.0018, \\ D_A(z = 0.35)/r_s(z_d) &= 6.60 \pm 0.26, \\ r &= 0.0604. \end{aligned} \quad (24)$$

where  $r$  is the normalized correlation coefficient between  $H(z = 0.35)r_s(z_d)/c$  and  $D_A(z = 0.35)/r_s(z_d)$ , and  $r_s(z_d)$  is the sound horizon at the drag epoch given by Eqs. (13) and (17).

In a similar analysis using the CMASS galaxy sample from BOSS, Chuang et al. [51] found that

$$\begin{aligned} H(z = 0.57)r_s(z_d)/c &= 0.0454 \pm 0.0031, \\ D_A(z = 0.57)/r_s(z_d) &= 8.95 \pm 0.27, \\ r &= 0.4874. \end{aligned} \quad (25)$$

We marginalize over the growth rate measurement made by Chuang et al. [51] for a conservative approach.

GC data are included in our analysis by adding  $\chi_{GC}^2 = \chi_{GC1}^2 + \chi_{GC2}^2$ , with  $z_{GC1} = 0.35$  and  $z_{GC2} = 0.57$ , to  $\chi^2$  of a given model. Note that

$$\chi_{GCi}^2 = \Delta p_i [C_{GC}^{-1}(p_i, p_j)] \Delta p_j, \quad \Delta p_i = p_i - p_i^{data}, \quad (26)$$

where  $p_1 = H(z_{GCi})r_s(z_d)/c$  and  $p_2 = D_A(z_{GCi})/r_s(z_d)$ , with  $i = 1, 2$ .

### III. RESULTS

As mentioned above, in this paper we consider three simplest models:  $\Lambda$ CDM,  $w$ CDM, and CPL. To explore the evolution of color-luminosity parameter  $\beta$ , we study the case of constant  $\alpha$  and linear  $\beta(z) = \beta_0 + \beta_1 z$ ; for comparison, the case of constant  $\alpha$  and constant  $\beta$  is also taken into account.

We perform an MCMC likelihood analysis [61] to obtain  $\mathcal{O}(10^6)$  samples for each set of results presented in this paper. We assume flat priors for all the parameters, and allow ranges of the parameters wide enough such that further increasing the allowed ranges has no impact on the results. The chains typically have worst e-values (the variance(mean)/mean(variance) of 1/2 chains) much smaller than 0.01, indicating convergence.

In the following, we will discuss the results given by the SNe-only and the SNe+CMB+GC data, respectively.

#### A. SNe-only cases

In this subsection, we discuss the results given by the SNe-only data. Notice that the Hubble constant  $h$  has been marginalized during the  $\chi^2$  fitting process of SNe Ia,

so we only need to consider six free parameters, including  $\alpha$ ,  $\beta_0$ ,  $\beta_1$ ,  $\Omega_m$ ,  $w_0$ , and  $w_1$  (two parameters for the equation of state  $w(z)$ ). In Table I, we list the fitting results for various constant  $\beta$  and linear  $\beta(z)$  cases, where only SNe data are used. The most obvious feature of this table is that varying  $\beta$  can significantly improve the fitting results. Moreover, this conclusion is insensitive to the DE models: for all the models considered here, adding a parameter of  $\beta$  can reduce the best-fit values of  $\chi^2$  by  $\sim 35$ . In contrast, adding  $w$  as a parameter or considering the evolution of  $w$  can only reduce the values of  $\chi^2$  by 1 or 2. This shows the importance of considering  $\beta$ 's evolution in the cosmology-fits.

Firstly, we discuss the results of the  $\Lambda$ CDM model. In Fig. 1, using SNe-only data, we plot the joint 68% and 95% confidence contours for  $\{\beta_0, \beta_1\}$  (top panel), and the 68%, 95%, and 97% confidence constraints for  $\beta(z)$  (bottom panel), for the linear  $\beta(z)$  case. For comparison, we also show the best-fit result of constant  $\beta$  case on the bottom panel. The top panel shows that  $\beta_1 > 0$  at a high confidence level (CL), while the bottom panel shows that  $\beta(z)$  rapidly increases with  $z$ . Moreover, based on this figure, we find the deviation of  $\beta$  from a constant at  $5\sigma$  CL. This result is similar to Figure 2 of [47], where a fixed cosmology background (a  $\Lambda$ CDM model with  $\Omega_m = 0.26$ ) was used in that paper.

Now, we study the effects of varying  $\beta$  on the parameter estimation of  $\Lambda$ CDM model. In Fig. 2, using SNe-only data, we plot the 1D marginalized probability distribution of  $\Omega_m$  for both the constant  $\beta$  and linear  $\beta(z)$  cases. We find that varying  $\beta$  yields a larger  $\Omega_m$ : the best-fit result for the constant  $\beta$  case is  $\Omega_m = 0.226$ , while best-fit result for the linear  $\beta(z)$  case is  $\Omega_m = 0.280$ . To make a direct comparison, we also plot the 1D distributions of  $\Omega_m$  given by the CMB+GC data, and find that the best-fit result for this case is  $\Omega_m = 0.287$ . Therefore, the result of linear  $\beta(z)$  case is much closer to that given by the CMB+GC data, compared to the case of treating  $\beta$  as a constant. This means that varying  $\beta$  is very helpful to reduce the tension between SNe and other cosmological observations.

Next, we discuss the results of the  $w$ CDM model and the CPL model. In Fig. 3, using SNe-only data, we plot the 68%, 95%, and 97% confidence constraints for  $\beta(z)$ , for the  $w$ CDM model (top panel) and the CPL model (bottom panel). Again, we find that for both the  $w$ CDM model and the CPL model,  $\beta$  deviates from a constant at  $5\sigma$  CL. Therefore, the evolution of  $\beta$  is insensitive to the models considered. Based on Table I, one can see that, for both the  $w$ CDM model and the CPL model, varying  $\beta$  yields a smaller  $\Omega_m$ , compared to the cases of assuming a constant  $\beta$ . This result is different from that of the  $\Lambda$ CDM model, and is also different from the results given by the SNe+CMB+GC data (see next subsection). This may be due to using SNe data alone still has difficulty to break the degeneracy between  $\Omega_m$  and  $w$ .

TABLE I: Fitting results for various constant  $\beta$  and linear  $\beta(z)$  cases, where only SNe data are used.

Parameters	$\Lambda$ CDM		$w$ CDM		CPL	
	Const $\beta$	Linear $\beta(z)$	Const $\beta$	Linear $\beta(z)$	Const $\beta$	Linear $\beta(z)$
$\alpha$	$1.425^{+0.109}_{-0.103}$	$1.410^{+0.106}_{-0.094}$	$1.427^{+0.108}_{-0.101}$	$1.410^{+0.103}_{-0.092}$	$1.427^{+0.106}_{-0.106}$	$1.415^{+0.096}_{-0.097}$
$\beta_0$	$3.259^{+0.110}_{-0.108}$	$1.457^{+0.370}_{-0.376}$	$3.256^{+0.114}_{-0.102}$	$1.439^{+0.398}_{-0.336}$	$3.265^{+0.104}_{-0.109}$	$1.499^{+0.300}_{-0.453}$
$\beta_1$	N/A	$5.061^{+1.064}_{-1.027}$	N/A	$5.112^{+0.970}_{-1.074}$	N/A	$4.939^{+1.256}_{-0.796}$
$\Omega_m$	$0.226^{+0.040}_{-0.036}$	$0.280^{+0.052}_{-0.052}$	$0.163^{+0.100}_{-0.147}$	$0.135^{+0.215}_{-0.009}$	$0.320^{+0.055}_{-0.310}$	$0.252^{+0.137}_{-0.242}$
$w_0$	N/A	N/A	$-0.858^{+0.219}_{-0.224}$	$-0.630^{+0.058}_{-0.268}$	$-0.778^{+0.235}_{-0.268}$	$-0.667^{+0.254}_{-0.240}$
$w_1$	N/A	N/A	N/A	N/A	$-3.619^{+4.370}_{-1.380}$	$-2.260^{+2.609}_{-2.739}$
$\chi^2_{min}$	420.075	385.203	419.658	383.591	419.054	383.144

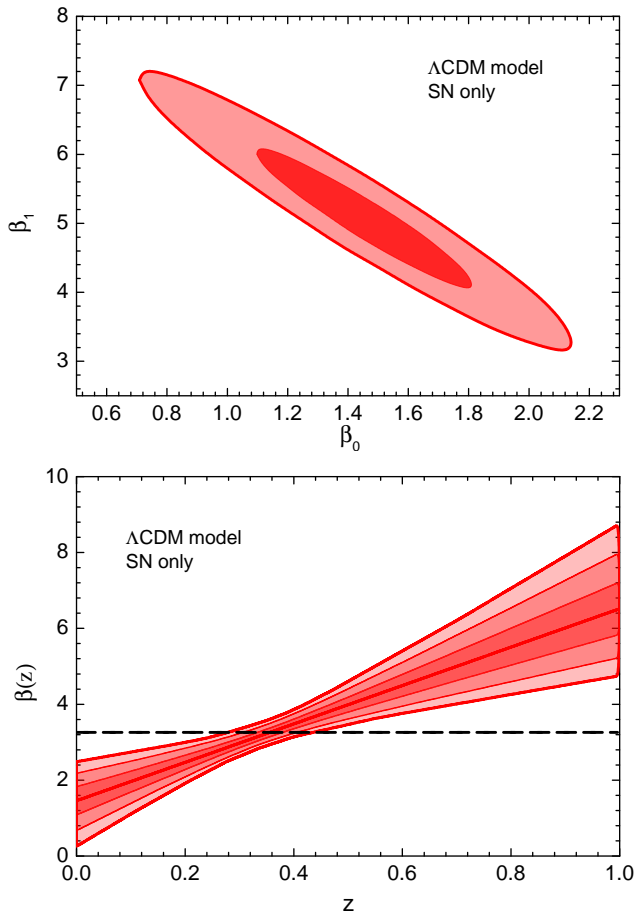


FIG. 1: The joint 68% and 95% confidence contours for  $\{\beta_0, \beta_1\}$  (top panel), and the 68%, 95%, and 97% confidence constraints for  $\beta(z)$  (bottom panel), given by the SNe-only data, for the  $\Lambda$ CDM model. For comparison, the best-fit result of constant  $\beta$  case is also shown on the bottom panel.

### B. SNe+CMB+GC cases

In this subsection, we discuss the results given by the SNe+CMB+GC data. It should be mentioned that, in order to use the Planck distance priors data, three new model parameters, including  $h$ ,  $\omega_b$ , and  $\Omega_k$ , must be added. In Table II, we list the fitting results for various constant  $\beta$  and linear  $\beta(z)$  cases, where the

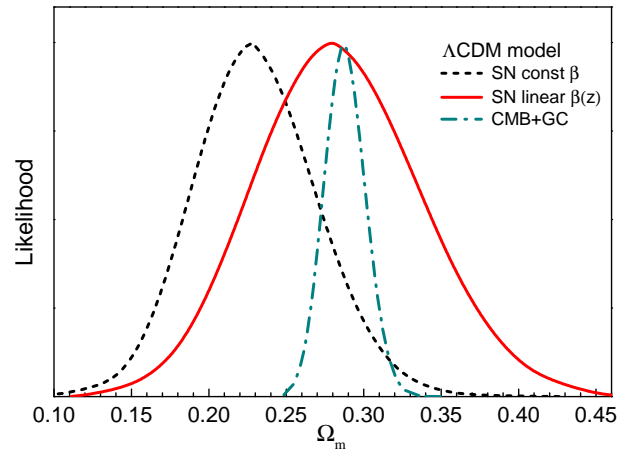


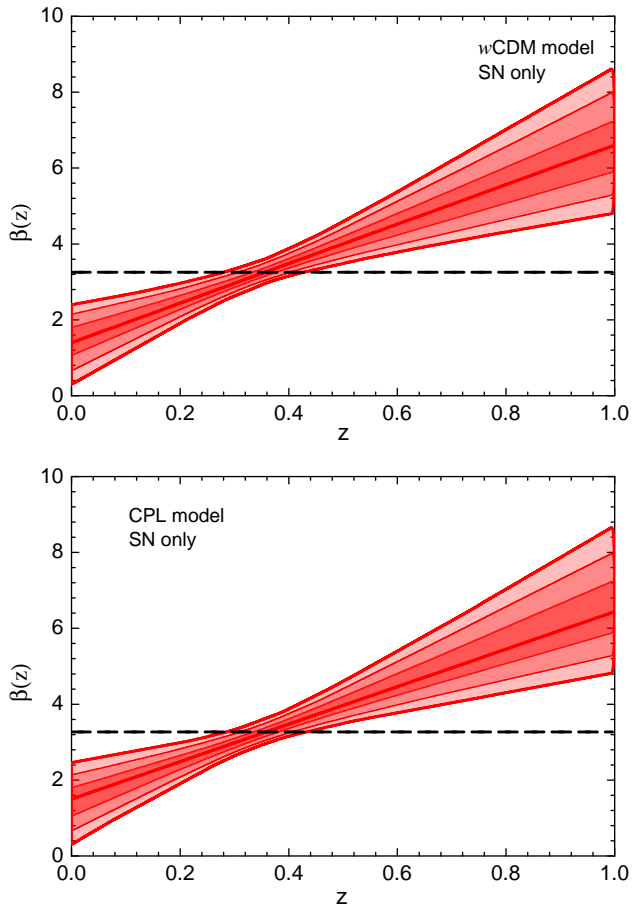
FIG. 2: The 1D marginalized probability distribution of  $\Omega_m$ , given by the SNe-only data, for the  $\Lambda$ CDM model. Both the results of constant  $\beta$  and linear  $\beta(z)$  cases are presented. The corresponding results given by the CMB+GC data are also shown for comparison.

SNe+CMB+GC data are used. Again, we find that varying  $\beta$  can significantly improve the fitting results. For all the DE models, adding a parameter of  $\beta$  can reduce the best-fit values of  $\chi^2$  by  $\sim 35$ , showing this conclusion is insensitive to the DE models. In contrast, adding  $w$  as a parameter or considering the evolution of  $w$  does not have significant impact on the fitting results. Therefore, it is very necessary and important to consider the evolution of  $\beta$  in the cosmology-fits.

Let us discuss the effects of varying  $\beta$  on various DE models in detail. In Fig. 4, using the SNe+CMB+GC data, we plot the 1D marginalized probability distribution of  $\Omega_m$  (top panel), and the joint 68% and 95% confidence contours for  $\{\Omega_m, h\}$  (bottom panel), for the  $\Lambda$ CDM model. From the top panel, we see that varying  $\beta$  yields a larger  $\Omega_m$ : the best-fit value of  $\Omega_m$  for the constant  $\beta$  case is 0.281, while best-fit value of  $\Omega_m$  for the linear  $\beta(z)$  case is 0.287. To make a direct comparison, we also plot the 1D distributions of  $\Omega_m$  given by the CMB+GC data. It is clear that the 1D distribution of  $\Omega_m$  for the linear  $\beta(z)$  case is closer to that given by the CMB+GC data. So we can conclude that varying  $\beta$  is very helpful to reduce the tension between SNe and other cosmological observations. This conclusion is consistent

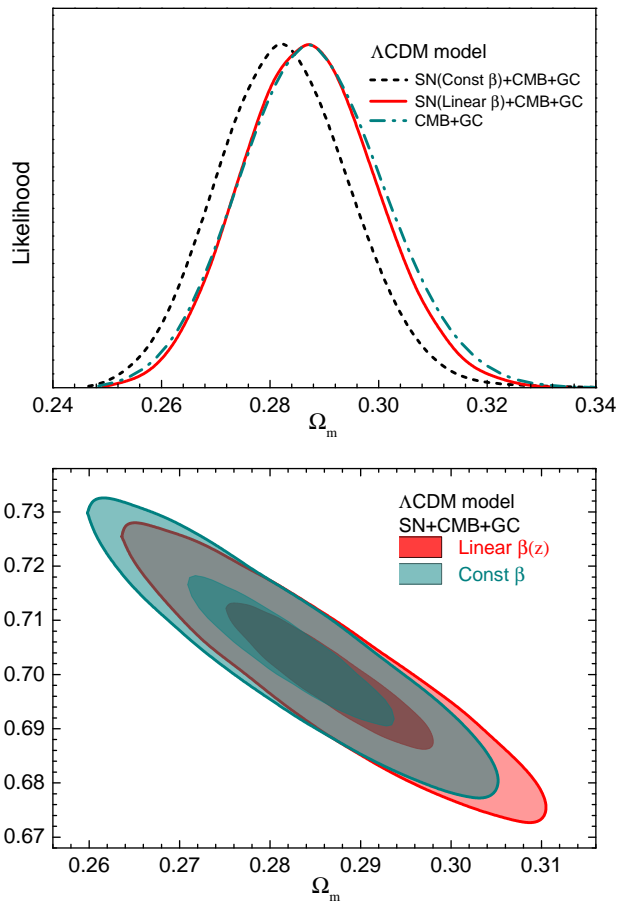
TABLE II: Fitting results for various constant  $\beta$  and linear  $\beta(z)$  cases, where the SNe+CMB+GC data are used.

Parameters	$\Lambda$ CDM		$w$ CDM		CPL	
	Const $\beta$	Linear $\beta(z)$	Const $\beta$	Linear $\beta(z)$	Const $\beta$	Linear $\beta(z)$
$\alpha$	$1.429^{+0.099}_{-0.111}$	$1.421^{+0.093}_{-0.100}$	$1.433^{+0.095}_{-0.108}$	$1.425^{+0.086}_{-0.105}$	$1.438^{+0.090}_{-0.103}$	$1.421^{+0.079}_{-0.093}$
$\beta_0$	$3.249^{+0.109}_{-0.106}$	$1.400^{+0.394}_{-0.326}$	$3.253^{+0.109}_{-0.099}$	$1.493^{+0.300}_{-0.420}$	$3.269^{+0.099}_{-0.104}$	$1.478^{+0.258}_{-0.389}$
$\beta_1$	N/A	$5.208^{+0.890}_{-1.074}$	N/A	$4.960^{+1.089}_{-0.798}$	N/A	$5.012^{+1.100}_{-0.735}$
$\Omega_m$	$0.281^{+0.013}_{-0.010}$	$0.287^{+0.011}_{-0.013}$	$0.270^{+0.014}_{-0.013}$	$0.286^{+0.013}_{-0.016}$	$0.275^{+0.012}_{-0.013}$	$0.280^{+0.013}_{-0.015}$
$h$	$0.704^{+0.013}_{-0.014}$	$0.698^{+0.015}_{-0.012}$	$0.719^{+0.016}_{-0.018}$	$0.698^{+0.021}_{-0.016}$	$0.714^{+0.019}_{-0.015}$	$0.706^{+0.020}_{-0.016}$
$\omega_b$	$0.02233^{+0.00028}_{-0.00030}$	$0.02226^{+0.00030}_{-0.00026}$	$0.02229^{+0.00028}_{-0.00028}$	$0.02235^{+0.00022}_{-0.00034}$	$0.02228^{+0.00027}_{-0.00028}$	$0.02229^{+0.00023}_{-0.00028}$
$\Omega_k$	$0.0031^{+0.0035}_{-0.0035}$	$0.0024^{+0.0037}_{-0.0033}$	$0.0009^{+0.0031}_{-0.0045}$	$0.0019^{+0.0051}_{-0.0036}$	$-0.0076^{+0.0053}_{-0.0033}$	$-0.0093^{+0.0054}_{-0.0029}$
$w_0$	N/A	N/A	$-1.091^{+0.064}_{-0.085}$	$-1.002^{+0.078}_{-0.075}$	$-0.783^{+0.162}_{-0.226}$	$-0.619^{+0.190}_{-0.209}$
$w_1$	N/A	N/A	N/A	N/A	$-2.180^{+1.424}_{-1.097}$	$-3.059^{+1.610}_{-1.394}$
$\chi^2_{min}$	423.922	387.077	422.296	387.041	420.022	383.826

FIG. 3: The 68%, 95%, and 97% confidence constraints for  $\beta(z)$ , given by the SNe-only data, for the  $w$ CDM model (top panel) and the CPL model (bottom panel). For comparison, the best-fit results of constant  $\beta$  cases are also shown.

with that of Fig. 2. From the bottom panel, we see that varying  $\beta$  will also yield a smaller  $h$ : the best-fit value of  $h$  for the constant  $\beta$  case is 0.704, while best-fit value of  $h$  for the linear  $\beta(z)$  case is 0.698. In addition, it is clear that  $\Omega_m$  and  $h$  are anti-correlated.

Then, we turn to the  $w$ CDM model. In Fig. 5, using the SNe+CMB+GC data, we plot the joint 68% and

FIG. 4: The 1D marginalized probability distribution of  $\Omega_m$  (top panel), and the joint 68% and 95% confidence contours for  $\{\Omega_m, h\}$  (bottom panel), given by the SNe+CMB+GC data, for the  $\Lambda$ CDM model. Both the results of constant  $\beta$  and linear  $\beta(z)$  cases are shown. The corresponding results given by the CMB+GC data are also shown for comparison.

95% confidence contours for  $\{\Omega_m, h\}$  (top panel) and  $\{\Omega_m, w_0\}$  (bottom panel), for the  $w$ CDM model. From the top panel, we see that varying  $\beta$  yields a larger  $\Omega_m$  and a smaller  $h$ : the best-fit results for the constant  $\beta$  case are  $\Omega_m = 0.270$  and  $h = 0.719$ , while best-fit results

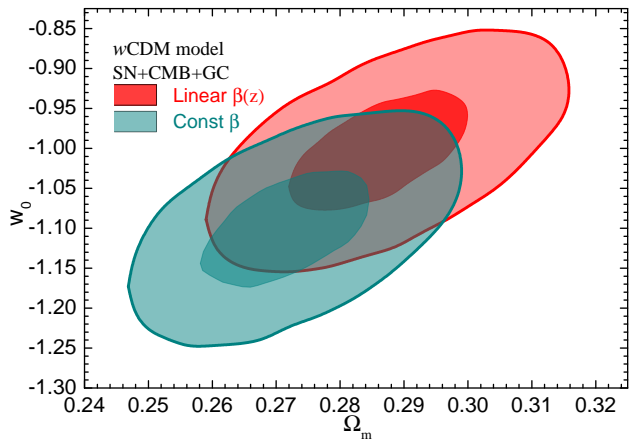
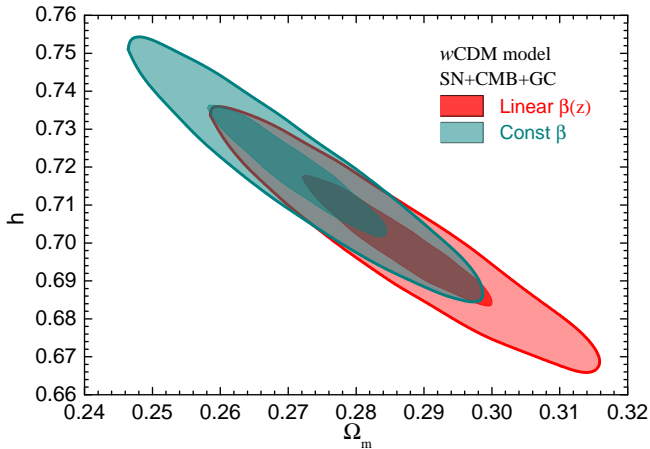


FIG. 5: The joint 68% and 95% confidence contours for  $\{\Omega_m, h\}$  (top panel) and  $\{\Omega_m, w_0\}$  (bottom panel), given by the SNe+CMB+GC data, for the  $w$ CDM model. Both the results of constant  $\beta$  and linear  $\beta(z)$  cases are shown for comparison.

for the linear  $\beta(z)$  case are  $\Omega_m = 0.286$  and  $h = 0.698$ . In addition,  $\Omega_m$  and  $h$  are anti-correlated. This is consistent with the case of the  $\Lambda$ CDM model. The bottom panel shows that varying  $\beta$  will also yield a large  $w_0$ : the best-fit value of  $w_0$  for the constant  $\beta$  case is  $-1.091$ , while best-fit value of  $w_0$  for the linear  $\beta(z)$  case is  $-1.002$ . Notice that after considering the evolution of  $\beta$ , the results of the  $w$ CDM model are closer to that of the  $\Lambda$ CDM model. In addition,  $\Omega_m$  and  $w_0$  are also in positive correlation.

Next, we discuss the CPL model. In Fig. 6, using the SNe+CMB+GC data, we plot the joint 68% and 95% confidence contours for  $\{\Omega_m, h\}$  (top panel) and  $\{\Omega_m, w_0\}$  (bottom panel), for the CPL model. Again, we see from the top panel that varying  $\beta$  yields a larger  $\Omega_m$  and a smaller  $h$ : the best-fit results for the constant  $\beta$  case are  $\Omega_m = 0.275$  and  $h = 0.714$ , while best-fit results for the linear  $\beta(z)$  case are  $\Omega_m = 0.280$  and  $h = 0.706$ . In addition,  $\Omega_m$  and  $h$  are also anti-correlated. The bottom panel shows that varying  $\beta$  will also yield a larger  $w_0$ : the best-fit value of  $w_0$  for the constant  $\beta$  case is  $-0.783$ , while best-fit value of  $w_0$  for the linear  $\beta(z)$  case

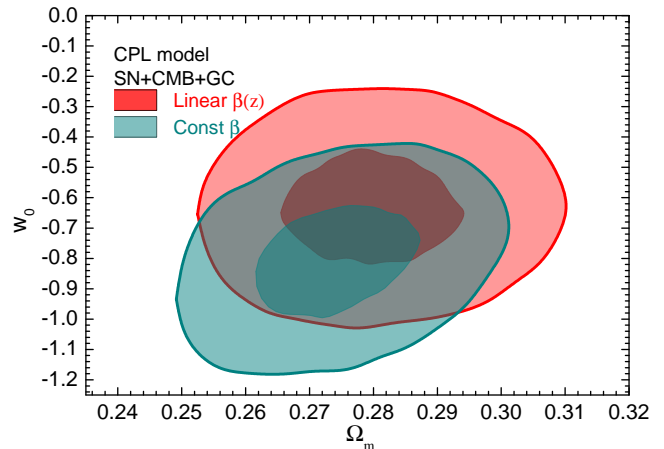
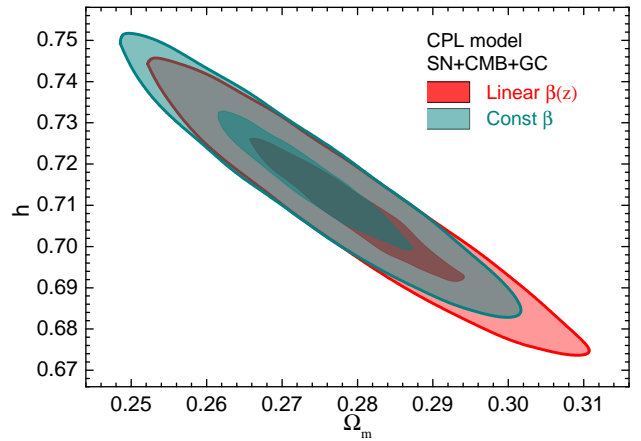


FIG. 6: The joint 68% and 95% confidence contours for  $\{\Omega_m, h\}$  (top panel) and  $\{\Omega_m, w_0\}$  (bottom panel), given by the SNe+CMB+GC data, for the CPL model. Both the results of constant  $\beta$  and linear  $\beta(z)$  cases are shown for comparison.

is  $-0.619$ . These results are consistent with the cases of the  $\Lambda$ CDM model and the  $w$ CDM model. To make a direct comparison, we also study the CPL model using the CMB+GC data, and find that the best-fit results for this case are  $\Omega_m = 0.282$ ,  $h = 0.709$  and  $w_0 = -0.712$ . It is clear that the fitting results for the linear  $\beta(z)$  case are much closer to that given by the CMB+GC data, compared to the case of treating  $\beta$  as a constant. This indicates that the conclusion of Figs. 2 and 4 is insensitive to the DE models considered.

Finally, we discuss the effects of varying  $\beta$  on equation of state (EOS)  $w(z)$  of the CPL model. In Fig. 7, using the SNe+CMB+GC data, we plot the joint 68% and 95% confidence contours for  $\{w_0, w_1\}$  (top panel), and the 68% and 95% confidence constraints for  $w(z)$  (bottom panel), for the CPL model. The top panel shows that varying  $\beta$  yields a larger  $w_0$  and a smaller  $w_1$ , while  $w_0$  and  $w_1$  are anti-correlated. The bottom panel shows that after considering the evolution of  $\beta$ , EOS  $w(z)$  of the CPL model will decrease faster with redshift  $z$ .

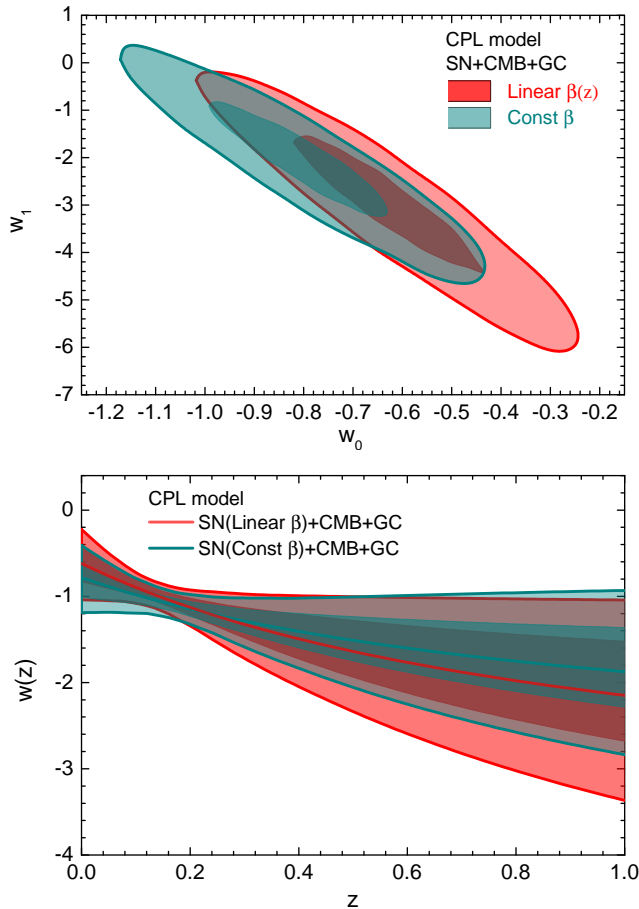


FIG. 7: The joint 68% and 95% confidence contours for  $\{w_0, w_1\}$  (top panel), and the 68% and 95% confidence constraints for  $w(z)$  (bottom panel), given by the SNe+CMB+GC data, for the CPL model. Both the results of constant  $\beta$  and linear  $\beta(z)$  cases are shown for comparison.

#### IV. DISCUSSION AND SUMMARY

One of the most important systematic uncertainties for SNe Ia is the potential SNe evolution, i.e., the possibility of the evolution of  $\alpha$  and  $\beta$  with redshift  $z$ . This issue had been studied for both the SDSS [40] and the Union2.1 [46] SNe samples. In [47], Wang & Wang studied this issue by using the SNLS3 data and MCMC technique. They found that  $\alpha$  is still consistent with a constant, but there is a strong evidence for the evolution of  $\beta$ . It should be stressed that this conclusion is insensitive to the lightcurve fitters used to derive the SNLS3 sample, or

the functional form of  $\beta(z)$  assumed [47]. It is clear that a time-varying  $\beta$  will have significant impact on parameter estimation, which had not been discussed in detail in [47].

In this paper, by adopting a constant  $\alpha$  and a linear  $\beta(z) = \beta_0 + \beta_1 z$ , we have further explored the evolution of  $\beta$  and its effects on parameter estimation. To perform the cosmology-fits, we have considered three simplest DE models:  $\Lambda$ CDM,  $w$ CDM, and CPL. For comparison, we have also taken into account the Planck distance priors data, as well as the latest GC data extracted from SDSS DR7 [50] and BOSS[51].

We find that, for all the models,  $\beta$  deviates from a constant at  $5\sigma$  confidence levels (see Figs. 1 and 3). Moreover, we find that varying  $\beta$  can significantly improve the fitting results: adding a parameter of  $\beta$  can reduce the best-fit values of  $\chi^2$  by  $\sim 35$  (see Tables I and II). This indicates that the evolution of  $\beta$  is insensitive to the DE models considered, and should be taken into account seriously in the cosmology-fits.

We find that, using the SNLS3 data alone, varying  $\beta$  yields a larger  $\Omega_m$  for the  $\Lambda$ CDM model (see Fig. 2); using the combined SNLS3+CMB+GC data, varying  $\beta$  yields a larger  $\Omega_m$  and a smaller  $h$  for all the model (see Figs. 4, 5 and 6). For the  $w$ CDM model, varying  $\beta$  will also yield a larger  $w_0$  (see Fig. 5); for the CPL model, varying  $\beta$  yields a larger  $w_0$  and a smaller  $w_1$  (see Fig. 7). Moreover, these results are closer to those given by the CMB+GC data, compared to the cases of treating  $\beta$  as a constant. This shows that considering the evolution of  $\beta$  can reduce the tension between supernova and other cosmological observations.

In this paper, only three simplest DE models are considered. It will be interesting to study the effects of varying  $\beta$  on parameter estimation of other DE models. In addition, some other factors, such as the evolution of  $\sigma_{int}$  [52], may also cause the systematic uncertainties of SNe Ia. These issues will be studied in future works.

Our understanding of the systematic uncertainties of SNe Ia will improve as larger and more uniform sets of SNe become available from future surveys [62–64].

**Acknowledgments** We are grateful to Alex Conley for providing us with the SNLS3 covariance matrices that allow redshift-dependent  $\alpha$  and  $\beta$ . We acknowledge the use of CosmoMC. This work is supported by the National Natural Science Foundation of China (Grants No. 10975032 and No. 11175042) and by the National Ministry of Education of China (Grants No. NCET-09-0276 and No. N120505003).

[1] A. G. Riess *et al.*, *AJ*. **116**, 1009 (1998); S. Perlmutter *et al.*, *ApJ*. **517**, 565 (1999).  
 [2] D. N. Spergel *et al.*, *ApJS* **148**, 175 (2003); C. L. Bennet *et al.*, *ApJS*. **148**, 1 (2003); D. N. Spergel *et al.*, *ApJS* **170**, 377 (2007); L. Page *et al.*, *ApJS* **170**, 335 (2007); G. Hinshaw *et al.*, *ApJS* **170**, 263 (2007).

[3] M. Tegmark *et al.*, *Phys. Rev. D* **69**, 103501 (2004); *ApJ* **606**, 702 (2004); *Phys. Rev. D* **74**, 123507 (2006).  
 [4] E. Komatsu *et al.*, *ApJS*. **180**, 330 (2009); E. Komatsu *et al.*, *ApJS*. **192**, 18 (2011).  
 [5] W. J. Percival *et al.*, *MNRAS* **401**, 2148 (2010); A. G. Sanchez, *et al.*, arXiv:1203.6616, *MNRAS* accepted.



- [6] M. Drinkwater *et al.*, MNRAS **401**, 1429 (2010); C. Blake *et al.*, arXiv:1108.2635, MNRAS accepted.
- [7] A. G. Riess *et al.*, ApJ **730**, 119 (2011).
- [8] P. J. E. Peebles and B. Ratra, ApJ **325**, L17 (1988); C. Wetterich, Nucl. Phys. B **302**, 668 (1988); R. R. Caldwell, R. Dave and P. J. Steinhardt, Phys. Rev. Lett. **80**, 1582 (1998); I. Zlatev, L. Wang and P. J. Steinhardt, Phys. Rev. Lett. **82**, 896 (1999).
- [9] R. R. Caldwell, Phys. Lett. B **545**, 23 (2002); S. M. Carroll, M. Hoffman and M. Trodden, Phys. Rev. D **68**, 023509 (2003); R. R. Caldwell, M. Kamionkowski and N. N. Weinberg, Phys. Rev. Lett. **91**, 071301 (2003).
- [10] C. Armendariz-Picon, T. Damour and V. Mukhanov, Phys. Lett. B **458**, 209 (1999); C. Armendariz-Picon, V. Mukhanov and P. J. Steinhardt, Phys. Rev. D **63**, 103510 (2001); T. Chiba, T. Okabe and M. Yamaguchi, Phys. Rev. D **62**, 023511 (2000).
- [11] A. Y. Kamenshchik, U. Moschella and V. Pasquier, Phys. Lett. B **511**, 265 (2001); M. C. Bento, O. Bertolami and A. A. Sen, Phys. Rev. D **66**, 043507 (2002).
- [12] T. Padmanabhan, Phys. Rev. D **66**, 021301 (2002); J. S. Bagla, H. K. Jassal, and T. Padmanabhan, Phys. Rev. D **67**, 063504 (2003).
- [13] M. Li, Phys. Lett. B **603**, 1 (2004); Q. G. Huang and M. Li, JCAP **08**, 013 (2004). X. Zhang and F. Q. Wu, Phys. Rev. D **72**, 043524 (2005); Phys. Rev. D **76**, 023502 (2007); M. Li, C. S. Lin and Y. Wang, JCAP **05**, 023 (2008); M. Li, X. D. Li, S. Wang and X. Zhang, JCAP **06**, 036 (2009); M. Li *et al.*, JCAP **12**, 014 (2009); Y. H. Li, S. Wang, X. D. Li and X. Zhang, JCAP **02**, 033 (2013); M. Li, X. D. Li, Y. Z. Ma, X. Zhang and Z. H. Zhang, JCAP **09**, 021 (2013).
- [14] H. Wei, R. G. Cai, and D. F. Zeng, Class. Quant. Grav. **22**, 3189 (2005); H. Wei, and R. G. Cai, Phys. Rev. D **72**, 123507 (2005); H. Wei, N. Tang, and S. N. Zhang, Phys. Rev. D **75**, 043009 (2007).
- [15] W. Zhao and Y. Zhang, Class. Quant. Grav. **23**, 3405 (2006); T. Y. Xia and Y. Zhang, Phys. Lett. B **656**, 19 (2007); S. Wang, Y. Zhang and T. Y. Xia, JCAP **10**, 037 (2008); S. Wang and Y. Zhang, Phys. Lett. B **669**, 201 (2008).
- [16] K. Freese *et al.*, Nucl. Phys. B **287**, 797 (1987); A. Linde, in *Three hundred years of gravitation*, (Eds.: Hawking, S.W. and Israel, W., Cambridge Univ. Press, 1987), 604; J. A. Frieman, C. T. Hill, A. Stebbins, and I. Waga, Phys. Rev. Lett. **75**, 2077 (1995); M. Chevallier and D. Polarski, Int. J. Mod. Phys. D **10**, 213 (2001); E. V. Linder, Phys. Rev. Lett. **90**, 091301 (2003); D. Huterer and G. Starkman, Phys. Rev. Lett. **90**, 031301 (2003); D. Huterer and A. Cooray, Phys. Rev. D **71**, 023506 (2005); A. Shafieloo, V. Sahni and A. A. Starobinsky, Phys. Rev. D **80**, 101301(R) (2009).
- [17] Y. Wang and M. Tegmark, Phys. Rev. Lett. **92**, 241302 (2004); Y. Wang, and K. Freese, Phys. Lett. B **632**, 449 (2006); Y. Wang and P. Mukherjee, ApJ **650**, 1 (2006); Y. Wang and P. Mukherjee, Phys. Rev. D **76**, 103533 (2007); Y. Wang, Phys. Rev. D **78**, 123532 (2008).
- [18] Y. Wang and M. Tegmark, Phys. Rev. D **71**, 103513 (2005);
- [19] Q. G. Huang, M. Li, X. D. Li and S. Wang, Phys. Rev. D **80**, 083515 (2009); S. Wang, X. D. Li and M. Li, Phys. Rev. D **82**, 103006 (2010); M. Li, X. D. Li and X. Zhang, Sci. China Phys. Mech. Astron. **53**, 1631 (2010); S. Wang, X. D. Li and M. Li, Phys. Rev. D **83**, 023010 (2011); X. D. Li *et al.*, JCAP **07**, (2011) 011; J. Z. Ma and X. Zhang, Phys. Lett. B **699**, 233 (2011); H. Li and X. Zhang, Phys. Lett. B **713**, 160 (2012); X. D. Li, S. Wang, Q. G. Huang, X. Zhang and M. Li, Sci. China Phys. Mech. Astron. **55**, 1330 (2012).
- [20] V. Sahni and S. Habib, Phys. Rev. Lett. **81**, 1766 (1998).
- [21] L. Parker and A. Raval, Phys. Rev. D **60**, 063512 (1999).
- [22] G. Dvali, G. Gabadadze and M. Porrati, Phys. Lett. B **485**, 208 (2000).
- [23] S. Nojiri, S. D. Odintsov, and M. Sasaki, Phys. Rev. D **71**, 123509 (2005).
- [24] A. Nicolis, R. Rattazzi, and E. Trincherini, Phys. Rev. D **79**, 064036 (2009).
- [25] W. Hu and I. Sawicki, Phys. Rev. D **76**, 064004 (2007); A. A. Starobinsky, J. Exp. Theor. Phys. Lett. **86**, (2007) 157.
- [26] G. R. Bengochea and R. Ferraro, Phys. Rev. D **79**, 124019 (2009); E. V. Linder, Phys. Rev. D **81**, (2010) 127301.
- [27] T. Harko, F. S. N. Lobo, S. Nojiri and S. D. Odintsov, Phys. Rev. D **84**, 024020 (2011).
- [28] E. J. Copeland, M. Sami and S. Tsujikawa, Int. J. Mod. Phys. D **15**, 1753 (2006).
- [29] J. Frieman, M. Turner and D. Huterer, Ann. Rev. Astron. Astrophys **46**, 385 (2008).
- [30] E. V. Linder, Rept. Prog. Phys. **71**, 056901 (2008).
- [31] R. R. Caldwell and M. Kamionkowski, Ann. Rev. Nucl. Part. Sci. **59**, 397 (2009).
- [32] J.-P. Uzan, arXiv:0908.2243.
- [33] S. Tsujikawa, arXiv:1004.1493.
- [34] S. Nojiri and S. D. Odintsov, Phys. Rept. **505**, 59 (2011).
- [35] M. Li, X. D. Li, S. Wang and Y. Wang, Commun. Theor. Phys. **56**, 525 (2011).
- [36] T. Clifton, P. G. Ferreira, A. Padilla and C. Skordis, Phys. Rept. **513**, 1 (2012).
- [37] Y. Wang, *Dark Energy*, Wiley-VCH (2010).
- [38] M. Kowalski, *et al.*, ApJ **686**, 749 (2008).
- [39] M. Hicken, *et al.*, ApJ **700**, 1097 (2009); M. Hicken, *et al.*, ApJ **700**, 331 (2009).
- [40] R. Kessler, *et al.*, ApJS **185**, 32 (2009).
- [41] R. Amanullah, *et al.*, ApJ **716**, 712 (2010).
- [42] N. Suzuki, *et al.*, ApJ **746**, 85 (2012).
- [43] J. Guy, *et al.*, A&A, **523**, 7 (2010).
- [44] A. Conley, *et al.*, ApJS **192** 1 (2011) – C11
- [45] M. Sullivan, *et al.*, arXiv:1104.1444.
- [46] G. Mohlabeng and J. Ralston, arXiv:1303.0580.
- [47] S. Wang and Y. Wang, Phys. Rev. D **88**, 043511 (2013).
- [48] M. Chevallier and D. Polarski, Int. J. Mod. Phys. D **10**, 213 (2001); E. V. Linder, Phys. Rev. Lett. **90**, 091301 (2003).
- [49] Y. Wang and S. Wang, Phys. Rev. D **88**, 043522 (2013).
- [50] C. H. Chuang and Y. Wang, MNRAS, **426**, 226 (2012).
- [51] C. H. Chuang, *et al.*, arXiv:1303.4486.
- [52] A. Kim, arXiv:1101.3513; J. Marriner, *et al.*, arXiv:1107.4631.
- [53] Y. Wang, ApJ **536**, 531 (2000).
- [54] Y. Wang and P. Mukherjee, ApJ **606**, 654 (2004).
- [55] Y. Wang, JCAP, **03**, 005 (2005).
- [56] Y. Wang, C. H. Chuang and P. Mukherjee, Phys. Rev. D **85**, 023517 (2012).
- [57] Y. Wang and P. Mukherjee, Phys. Rev. D, **76**, 103533 (2007).
- [58] Y. Wang, Phys. Rev. D **77**, 123525 (2008).
- [59] W. Hu and N. Sugiyama, ApJ, **471**, 542 (1996).

- [60] D. Eisenstein and W. Hu, *ApJ*, **496**, 605 (1998).  
[61] A. Lewis and S. Bridle, *Phys. Rev. D* **66**, 103511 (2002).  
[62] Y. Wang, *ApJ* **531**, 676 (2000).  
[63] A. Crotts, *et al.* (2005), astro-ph/0507043  
[64] D. Spergel, *et al.* (2013), arXiv1305.5422